Multiscale Characterization Framework for Sorption Enhanced Reaction Processes

Ankur Kapil, Shrikant A. Bhat, and Jhuma Sadhukhan
Center for Process Integration, School of Chemical Engineering and Analytical Science,
The University of Manchester, Manchester, M60 1QD, U.K.

DOI 10.1002/aic.11428
Published online February 26, 2008 in Wiley InterScience (www.interscience.wiley.com).

A multiscale simulation and characterization framework has been developed for sorption enhanced reaction processes with heterogeneous multifunctional catalysts with sorption properties. Particles with in situ catalytic and sorption functionalities have obvious advantages in achieving high-purity and productivity. These processes are strongly limited by diffusion inside particle. In order to tackle this problem a more detailed characterization at particle level is essential, which is the main objective here. A unified framework has been developed that integrates continuum model at bulk scale with the diffusion-reaction-sorption model at particle porous scale in a fixed-bed reactor. At bulk scale the objectives of purity and productivity are sensitive to various design and operating variables, such as wall temperature, bed voidage and feed compositions, etc. Two important particle level characteristics are also identified: distribution of catalyst and sorbent inside particles, and the ratio of pore radius to tortuosity. It has been demonstrated that considering detailed diffusivity model at porous level offers better insights into catalyst design and process intensification. Natural gas reforming reaction with sorption producing pure hydrogen for fuel cell and combustion applications has been used as a case study to establish the effectiveness of the methodology. © 2008 American Institute of Chemical Engineers *AIChE J,* 54: 1025–1036, 2008
Keywords: sorption enhanced reaction, multiscale design, multifunctional catalyst, porous diffusion, natural gas reforming, hydrogen

Introduction

Equilibrium driven reactions with integrated separation of one or more components are based on the application of the Le Chatelier's principle, and are targeted toward increasing productivity and purity of desired product through a more favorable reaction equilibrium.[1] This concept gives an additional degree of freedom in the design of multifunctional catalysts for intensifying processes. Various separation functionalities that can be incorporated in the reactor design include sorption, membrane separation, distillation, extraction, pervaporation, electrodialysis, etc.[2,3] Sorption enhanced reaction process offers some distinct advantages in terms of tolerance of materials to high-temperature and-pressure, wider range of availability of sorbents for a desired separation, and productivity of pure product.[4,5]

Within the last few years, several experiments and modeling studies have been done for sorption enhanced reaction process.[4,6–13] Here we have presented a novel methodology for multiscale simulation and characterization of heterogeneous catalytic sorption enhanced reaction processes, with sorbent and catalyst integrated in a single particle. We have selected steam methane reforming (SMR) reaction as a representative system for demonstrating the effectiveness of our methodology. This system has been widely studied using experimental, as well as modeling approaches. It is also an important area of research from a point of view of hydrogen economy and natural gas utilization in decarbonized hydro-

Correspondence concerning this article should be addressed to J. Sadhukhan at jhuma.sadhukhan@manchester.ac.uk.

gen production (with *in situ* carbon dioxide separation). Ding and Alpay[11] developed a laboratory scale homogeneous experimental system with catalyst and sorbent crushed and sieved to uniform fine particles that were packed into the reactor. They also developed pseudo-homogeneous model for representing the system. Obviously their model was limited to bulk scale. However, homogeneous model is a crude assumption, and such processes are not feasible for industrial scale reactor, due to large pressure drop for such an arrangement. Hufton et al.[4,5] conducted a bench-scale experiment with an admixture of catalyst, and a reversible chemisorbent in separate particles for SMR. Air Products[4,5,7] have demonstrated the concept of sorption enhanced reaction process for SMR on experimental and pilot plant scale. The experimental setup consists of a tubular reactor packed with different particles of CO_2 chemisorbent and SMR catalyst in equal weight ratio. However, so far, no experimental data are available on multifunctional particle systems.

At the same time there are significant attempts in theoretical studies on sorption enhanced reaction system. Xiu et al.[14] developed a theoretical model to describe fixed-bed sorption enhanced reaction process, which takes into account multicomponent and overall mass balance, energy balance for the bed-volume element, Ergun equation for pressure drop and nonlinear adsorption equilibrium isotherm coupled with SMR reaction equations. However, their model does not consider the effect of diffusion of reactants and products inside the particle. For slow diffusion and fast reaction this has a significant effect on the overall process. They extended their methodology by including a number of sections with different packing ratio of catalyst and adsorbent, and different subsection temperature.[15] Xiu et al.[16] further extended their methodology to account for intraparticle difusión for the two particle system of catalyst and adsorbent by including the component mass balance inside the particle. Wang and Rodrigues[13] developed a subsection simplified process model (isothermal and isobaric), based on the previous model by Xiu et al.[14,15] Their model consists of component and overall mass balance equations combined with reaction equilibrium and adsorption isotherm. The first section was the equilibrium conversion section, while the second section was the adsorption reforming section containing a mixture of catalyst and sorbent. They showed the effect of various operating parameters, such as steam to methane ratio, bed length, temperature, pressure, catalyst to adsorbent ratio, etc., on the process. Koumpouras et al.[17–19] developed a mathematical model, based on mass and energy balance inside the reactor and regenerator for a proposed new process in which pneumatically conveyed adsorbent particles are passed through a stationary SMR catalyst monolith. They assumed that the concentration gradients through the monolith and the catalyst wash coat are negligible.However, all these studies are restricted to cases with catalyst and sorbent present as different particles. In such cases the inter and intra mass transfer poses serious constraints in terms of intensifying sorptive reactors.[20] If catalyst and sorbent are integrated within single particle, the mass-transfer limitations can be reduced, and process intensification effects can be realized. Dietrich et al.[21] introduced the concept of spatial integration of catalytic and adsorptive functionality at the particle level. They have developed isothermal process scale model with only mass-transfer equations, and integrated that with particle-scale reaction-sorption model. However, their particle-scale model assumes fixed effective porous diffusivity, and no variation in diffusion through pores, due to molecular and molecule to pores interactions. Additionally, their isothermal process scale model will not be valid for many systems, such as SMR, where temperature variation is an important variable to control, due to coking and metal dusting problems, further illustrated in the case study. Rusten et al.[22] have introduced a more comprehensive heterogeneous model with mass, energy and momentum transfer equations at bulk scale and component balance, reaction and sorption kinetic model at particle scale, for SMR with multifunctional catalysts. The main thrust of this model is bulk scale characterization. The sorption enhanced reactions are diffusion limited with slow sorption kinetics. For these systems, velocity dependency on reaction and adsorption (namely momentum equation) is negligible, and its consideration is computationally significantly intensive as concluded by the authors. However, similar to Dietrich et al.[21] their particle-scale model does not consider detailed molecular and porous hindrance effects on particle diffusivity. It does not either involve particle-scale characterization, which is important for the design and performance of multifunctional particles.

First, development of heterogeneous multiscale simulation framework is imperative for decision making in sorption enhanced reaction processes with multifunctional catalysts that are proved to be more efficient than the cases with catalyst and sorbent in separate particles.[21] Second, the SMR and many such intensified processes have been determined to be strongly intraparticular diffusion controlled.[22] However, all previous works in heterogeneous modeling frameworks were restricted to the consideration of average effective diffusivities at particle level. If simulation and characterization of these systems can be extended to include detailed and fundamental particle-scale diffusivity models in a multiscale framework, important characterization parameters controlling particle-level diffusion can be determined and optimized to circumvent the mass transfer bottleneck. This is the main motivation of this work that has for the first time developed a comprehensive and fundamental particle-scale diffusion model in terms of molecule to molecule, and molecule to porous interaction parameters and integrated this into a heterogeneous multiscale simulation framework.

Design and optimization of sorption enhanced reaction processes requires manipulation of variables both at bulk, as well as at particle scales, such as temperature, bed voidage, feed composition, particle compositions and diffusivity inside particles, etc. In this research, we have studied the effect of temperature variations and spatial distribution of Thiele modulus on concentration profiles along reactor. Also, we have introduced a more generic particle-scale porous diffusion model, accounting for the effects of porous hindrance, as well as molecular interactions. The diffusivity inside particle is an important characterization variable for a better performance. In addition to allowing temperature variations and integration between bulk, and more detailed particle scales in our model, we have performed an analysis on the distribution of catalyst and sorbent in different particle designs:[21] (a) catalyst in core, and (b) sorbent in core in core-shell arrangements, and (c) uniform mixture of sorbent and catalyst, for

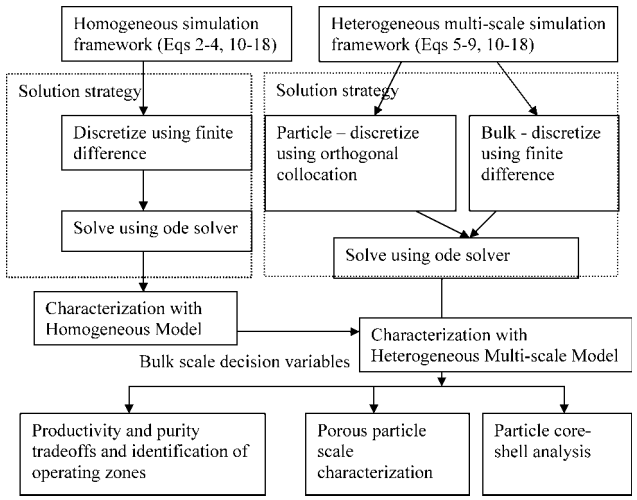

Figure 1. Methodology for characterization and simulation of adsorption enhanced reaction.

an optimal tradeoff between productivity and purity, as presented in the results and discussions section.

The content of this article is organized as follows: the following section provides the simulation framework developed in this study for sorption enhanced catalytic reaction processes. This includes both homogeneous, as well as heterogeneous multiscale simulation frameworks. The penultimate section highlights the results and discussions followed by conclusions in the end.

Methodology

This section presents a generic framework for the sorption enhanced processes with multi-functional catalyst-sorbent particles. The system under consideration is steam methane reforming (SMR)

$$CH_4 + H_2O \Leftrightarrow CO + 3H_2, \quad \Delta H_{R,I,298} = 206.2KJ/mol \quad \text{(I)}$$
$$CH_4 + 2H_2O \Leftrightarrow CO_2 + 4H_2, \quad \Delta H_{R,II,298} = 164.9KJ/mol \quad \text{(II)}$$
$$CO + H_2O \Leftrightarrow CO_2 + H_2, \quad \Delta H_{R,III,298} = -41.1KJ/mol \quad \text{(III)} \tag{1}$$

We have considered a fixed-bed reactor of length L, and dia. d_t, in developing (a) homogeneous simulation framework, and (b) heterogeneous multiscale simulation framework. An overview of the methodology is presented in Figure 1.

Homogeneous simulation framework [11]

The sorption enhanced reaction in this case is considered taking place in a homogeneous mixture of catalyst and sorbent. It is assumed that the concentration and temperature vary only in axial direction and are constant along the radial direction. The system is considered to be pseudo-homogeneous with perfect gas behavior, uniform voidage and catalyst and sorbent distribution. With these considerations, the material balance for each bulk gaseous specie i is a function of diffusional transfer (effective diffusivity D_L for the reactor), convection (axial velocity u), rates of reaction ($r_{cat,j}$), and sorption ($r_{ads,i}$), and is given as

$$\frac{\partial C_i}{\partial t} = \frac{D_L}{\varepsilon}\left(\frac{\partial^2 C_i}{\partial z^2}\right) - \frac{u}{\varepsilon}\frac{\partial C_i}{\partial z} - \frac{(1-\varepsilon)}{\varepsilon}\left[\rho_{ads} r_{ads,i} - \rho_{cat}\sum_{j=1}^{nrxn} v_{ij}\eta_j r_{cat,j}\right] \tag{2}$$

For a gas flow through a homogeneous bed of catalyst and sorbent, the energy balance across an element in bed volume exchanging heat through a wall is described by the following equation

$$\frac{\partial T}{\partial t} = \frac{1}{Cp_g\rho_g\varepsilon + Cp_s\rho_b}\left[\frac{\partial}{\partial z}\left(\lambda_z\frac{\partial T}{\partial z}\right) - Cp_g\rho_g u\frac{\partial}{\partial z}T - (1-\varepsilon)\sum_{i=1}^{nspc}\rho_{ads}\Delta H_{ads,i} r_{ads,i} + \rho_{cat}(1-\varepsilon)\sum_{j=1}^{nrxn}\eta_j\Delta H_{R,j} r_{cat,j} + \frac{4U}{d_t}(T_w - T)\right] \tag{3}$$

Boundary conditions are obtained from Danckwert's boundary conditions.[23] It is assumed that the molar flow (Eq. 4a), and heat flow (Eq. 4b) into a reactor is equal to the diffusion and conduction at the inlet of the reactor, respectively, and there is no change in the concentration and temperature at the outlet of the reactor (Eq. 4c and 4d, respectively)

$$\left(\varepsilon D_L\frac{\partial C_i}{\partial z}\right)_{z=0} = u(C_{f,i} - C_i) \tag{4a}$$
$$\left(\varepsilon\lambda_z\frac{\partial T}{\partial z}\right)_{z=0} = Cp_g uC(T_f - T) \tag{4b}$$
$$\left(\frac{\partial C_i}{\partial z}\right)_{z=L} = 0 \tag{4c}$$
$$\left(\frac{\partial T}{\partial z}\right)_{z=L} = 0 \tag{4d}$$

Solution strategy

These partial differential equations (PDEs), Eqs. 1–4, are converted to ordinary differential equations (ODEs), by the method of lines. Central finite difference scheme is used for discretizing the concentration and temperature profiles at all grid points. The process conditions and fixed parameters are specified in Appendix A.

Heterogeneous multiscale simulation framework

A two-scale model has been developed for the sorption enhanced reaction systems with multifunctional particles. The reactor bed contains a uniform distribution of multifunctional particles. The distribution of the catalyst and sorbent inside particles provides an important degree of freedom, which has been analyzed in this study.

Bulk scale model

The bulk phase component i balance equation is a function of diffusivity D_L, axial velocity u, same as in Eq. 2, and mass transfer at the surface of particle $N^*_{p,i}$

$$\frac{\partial C_i}{\partial t} = D_L \left(\frac{\partial^2 C_i}{\partial z^2}\right) - \frac{u}{\varepsilon}\left(\frac{\partial C_i}{\partial z}\right) + N^*_{p,i}\,\frac{3}{r_p}\frac{(1-\varepsilon)}{\varepsilon} \tag{5}$$

The energy equation over a control volume inside reactor is dependent on the average rate of reaction $\overline{R_{car,i}}$, and sorption $\overline{R_{ads,CO_2}}$ inside particles, and the heat exchange through the wall of reactor (overall heat-transfer coefficient U) for the control volume, and is given as

$$\frac{\partial T}{\partial t} = \frac{1}{Cp_g\rho_g\varepsilon + Cp_s\rho_b}\left[\frac{\partial}{\partial z}\left(\lambda_z\frac{\partial T}{\partial z}\right) - Cp_g\rho_g u\frac{\partial T}{\partial z} - (1-\varepsilon)(1-\varepsilon_p)\sum_{i=1}^{nspc}\rho_{ads}\Delta H_{ads,i}\overline{R_{ads,i}} + \rho_{cat}(1-\varepsilon)(1-\varepsilon_p) \times \sum_{j=1}^{nrxn}\eta_j\Delta H_{R,j}\rho_{cat}\overline{R_{cat,j}} + 4\frac{U}{d_t}(T_w - T)\right] \tag{6}$$

Boundary conditions for the bulk are same as in homogeneous simulation framework given by Danckwert's boundary condition,[23] Eq. 4.

Particle-scale model

The mass transfer inside a particle is given by the rate of diffusion at the surface of the particle

$$N^*_{p,i} = -d_i^{eff}\left.\frac{\partial C_i^p}{\partial r}\right|_{r=r_p} \tag{7}$$

Inside particles the dynamics of a specie is due to mass transfer, reaction $r_{cat,j}$, and sorption $r_{ads,j}$. The mass transfer is described using effective porous diffusivity d_i^{eff}. The contribution of reaction and sorption is weighted according to the volume fraction f^p_{ads} and f^p_{cat} of the corresponding functionalities, respectively. Hence, the component balance inside a particle is given by

$$\frac{\partial C_i^p}{\partial t} = \frac{d_i^{eff}}{\varepsilon_p}\left(\frac{1}{r^2}\frac{\partial^2(r^2C_i^p)}{\partial r^2}\right) - \frac{(1-\varepsilon_p)}{\varepsilon_p}\left[f^p_{ads}\rho_{ads}r_{ads,i} - \sum_{j=1}^{nrxn}\nu_{ij}\eta_j f^p_{cat}\rho_{cat}r_{cat,j}\right] \tag{8}$$

It is assumed that there are no mass-transfer limitations at the surface of particles, and, hence, the concentration at the surface of a particle is equal to the bulk concentration, Eq. 9a, and the concentration inside a particle is symmetric with the radius, Eq. 9b. The boundary conditions for particles are given as

$$At\ r = r_p: \quad C_i^p(r = r_p, z, t) = C_i(z, t) \tag{9a}$$

$$r = 0: \quad -d_i^{eff}\frac{\partial C_i^p}{\partial r} = 0 \tag{9b}$$

Solution strategy

The PDEs corresponding to particle-scale transport Eqs. 7–9 are converted into ODEs using the method of orthogonal collocation. Five orthogonal collocation points are taken inside a particle along its radius. Bulk differential Eqs. 5–6 are discretized by the method of finite difference. In this system, for a change in diffusivity, both axial and porous, there is a large variation and even instability in the solution (stiff equations). Therefore, stiff equation solver is used to solve these equations. These coupled set of ODEs for both particles and reactor are solved simultaneously using Matlab function ode15s, appropriate for a system with stiff equations. The process conditions and fixed parameters are specified in Appendix A.

Evaluation of Parameters

Parameters for Eqs. 1–9 are obtained as shown later.

Diffusivity inside particles is governed by the collisions between gas molecules and pore walls: molecular diffusivity d^e_{ij}, and Knudsen diffusivity d^e_{ki}, respectively as[24]

$$d_i^{eff} = \frac{1}{\left[\frac{1}{d^e_{ki}} + \frac{1}{\left(1-\frac{C_i^p P}{RT}\right)}\sum_{\substack{m=1\\ m\neq i}}^{nspc}\frac{C_m^p P}{RTd^e_{im}}\right]} \tag{10a}$$

Knudsen diffusion coefficient is a function of particle void fraction ε_p, radius of pore $\bar{r}$, and tortuosity τ_p[25]

$$d^e_{ki} = \frac{2\times\bar{r}}{3}\left[\frac{8RT}{\pi M_{w_i}}\right]^{0.5}\frac{\varepsilon_p}{\tau_p} \tag{10b}$$

The molecular diffusion inside a particle d^e_{im}, is dependent on temperature T, particle voidage ε_p, tortuosity τ_p, characteristic length σ_{im}, and diffusion collision integral Ω_{dim}, and Lennard-Jones energy ε_{im}[26]

$$d^e_{im} = \frac{10^3\times 0.00266T^{1.5}\varepsilon_p}{\tau_p P\sigma^2_{im}\Omega_{d\,im}}\left(\frac{1}{Mw_i} + \frac{1}{Mw_m}\right)^{0.5} \tag{10c}$$

$$\sigma_{im} = \frac{\sigma_i + \sigma_m}{2} \tag{10d}$$

$$\Omega_{d\,im} = \frac{1.6036}{\left(T^*\right)^{0.01561}} + \frac{0.193}{\exp\left(0.47635T^*\right)} + \frac{1.03587}{\exp\left(1.52996T^*\right)} + \frac{1.76474}{\exp\left(3.89411T^*\right)} \tag{10e}$$

$$T^* = \frac{kT}{\varepsilon_{im}} \tag{10f}$$

$$\varepsilon_{im} = \left(\varepsilon_i{}^*\varepsilon_m\right)^{0.5} \tag{10g}$$

For the heat transfer (Eq. 6) in heterogeneous multiscale simulation framework, the average rates of sorption and reaction are used, assuming that the temperature inside a particle will remain constant. Average rates are given by

$$\overline{R_{ads,i}} = \frac{3}{r_p{}^3}\int_{r=0}^{r_p} r^2 r_{ads,i}dr \quad i = 1,\ldots,nspc \tag{11a}$$

$$\overline{R_{cat,j}} = \frac{3}{r_p{}^3}\int_{r=0}^{r_p} r^2 r_{cat,j}dr \quad j = 1,..,nrxn \tag{11b}$$

The axial diffusion coefficient D_L, inside particles of average dia. d_p, is given by Edwards and Richardson[27] as

$$D_L = 0.73D_m + \frac{0.5ud_p}{1 + 9.49D_m/(ud_p)} \tag{12}$$

The pressure drop across a fixed-bed reactor is the function of bed porosity ε, and superficial velocity u, and is calculated using Ergun's equation[28]

$$\frac{\partial P}{\partial z} = -K_D u - K_V u^2 \tag{13a}$$

$$K_D = \frac{150\mu(1-\varepsilon)^2}{d_p^2\varepsilon^3} \tag{13b}$$

$$K_V = \frac{1.75(1-\varepsilon)}{d_p\varepsilon^3}\frac{PM}{RT} \tag{13c}$$

The effective axial conductivity λ_z is given by Yagi et al.[29]

$$\frac{\lambda_z}{\lambda_g} = \frac{\lambda_z^0}{\lambda_g} + 0.75(\mathrm{Pr})(\mathrm{Re}_p) \tag{14a}$$

$$\frac{\lambda_z^0}{\lambda_g} = \varepsilon + \frac{(1-\varepsilon)}{0.139\varepsilon - 0.0339 + 2/3(\lambda_g/\lambda_p)}0.75(\mathrm{Pr})(\mathrm{Re}_p) \tag{14b}$$

The bed void fraction ε is given by Dixon[30]

$$\varepsilon = 0.4 + 0.05\left(\frac{d_p}{d_t}\right) + 0.412\left(\frac{d_p}{d_t}\right)^2 \tag{15}$$

The linear driving force (LDF) model is used to describe the rate of sorption of species is given by Ding and Alpay[12]

$$r_{ads,i} = \frac{\partial \overline{q}_i}{\partial t} = k_{ads,i}\left(q_i^* - \overline{q}_i\right) \tag{16}$$

Here, the models for the specific reaction and sorption parameters are given for steam_methane reforming reaction under consideration, as follows $\overline{q}_{CO_2}$ is the sorbed-phase concentration of CO_2, and $q^*_{CO_2}$ is the equilibrium solid-phase concentration, and K_{ads,CO_2} is the mass-transfer coefficient, respectively

$$q^*_{CO_2} = \frac{m_{CO_2}b_{CO_2}P_{CO_2}}{(1 + b_{CO_2}P_{CO_2})} \tag{17a}$$

$$b_{CO_2} = 1.36\times10^{-4}\exp\left[\frac{17000}{R}\left(\frac{1}{T} - \frac{1}{673}\right)\right] \tag{17b}$$

$$k_{ads,CO_2} = \frac{15}{r_p^2}\frac{\varepsilon_p d_i^{eff}}{\varepsilon_p + \rho_p RT(\partial q^*_{CO_2}/\partial P_{CO_2})} \tag{17c}$$

The rates for the reactions in Eq 1. 1–3 are given by Xu and Froment[31] by the following expressions

$$r_{cat,I} = \frac{k(I)}{P_{H_2}^{2.5}}\left(P_{CH_4}P_{H_2O} - \frac{P_{H_2}^3 P_{CO}}{keq(I)}\right)/den^2 \tag{18a}$$

$$r_{cat,II} = \frac{k(II)}{P_{H_2}^{3.5}}\left(P_{CH_4}P_{H_2O}^2 - \frac{P_{H_2}^4 P_{CO_2}}{keq(II)}\right)/den^2 \tag{18b}$$

$$r_{cat,III} = \frac{k(III)}{P_{H_2}}\left(P_{CO}P_{H_2O} - \frac{P_{H_2}P_{CO_2}}{keq(III)}\right)/den^2 \tag{18c}$$

$$den = 1 + K_{CO}P_{CO} + K_{H_2}P_{H_2} + K_{CH_4}P_{CH_4} + \frac{K_{H_2O}P_{H_2O}}{P_{H_2}} \tag{18d}$$

Algorithm

The algorithm for homogeneous model can be described as

1. Given, P and T at initial time, evaluate the parameters, such as particle and axial diffusivities, heat-transfer coefficients, ergun equation coefficients using Eqs. 10, 12–15, respectively.
2. Discretize bulk concentration along the length (Eq. 2) to calculate the value of $\frac{dC_i}{dt}$
3. Discretize temperature along the length domain (Eq. 3) to calculate the value of $\frac{dT}{dt}$
4. Solve the resulting system of equations by ode15s solver in MATLAB over time *0- t* s with a time gap of 1s.
5. Bulk scale sensitivity analysis is carried out with respect to various decision variables, such as bed voidage, steam to Methane ratio, bed temperatures.

The algorithm for heterogeneous model can be described as:

1. Given C_i^p, C_i, P and T at initial time, evaluate the parameters, such as porous and axial diffusivity, heat-transfer coefficients, ergun equation coefficients, etc. using Eqs. 10, 12–15, respectively.
2. Discretize particle concentration along the radius (Eq. 7) to calculate the value of $\frac{dC_i^p}{dt}$
3. Discretize bulk concentration along the length (Eq. 5) to calculate the value of $\frac{dC_i}{dt}$
4. Discretize temperature along the length (Eq 8) to calculate the value of $\frac{dT}{dt}$
5. Solve the resulting system of equation by ode15s solver in MATLAB over time 0- t s, with a time gap of 1s.
6. Using the optimal values of bulk scale decision variables from step 5 of homogeneous simulation framework, the operating ranges of particle scale design variables, such as sorbent inside particles, particle voidage and diameter are established.
7. Finally, an analysis of the effect of particle level characterization parameters, such as the ratio of pore radius to tortuosity and Thiele modulus on the process objectives, such as productivity and purity is presented.

Results and Discussion

We have taken experimental results conducted by Ding and Alpay[11] on sorption enhanced steam methane reforming process in a homogeneous system as the reference case for our study. The process conditions are P = 4.45bar, T_f = 723K, T_w = 730K, u = 0.13m/s, L = 0.22m as given by Ding and Alpay.[11] The diameter of particles is 0.37mm, and the catalyst effectiveness factor η_j was assumed to be 0.8 for all the reactions. The parameters are listed in Appendix A.

Simulation Results with homogeneous and heterogeneous models

The homogeneous model in Eqs. 2–4 was used to validate the results against the experimental data on steam methane

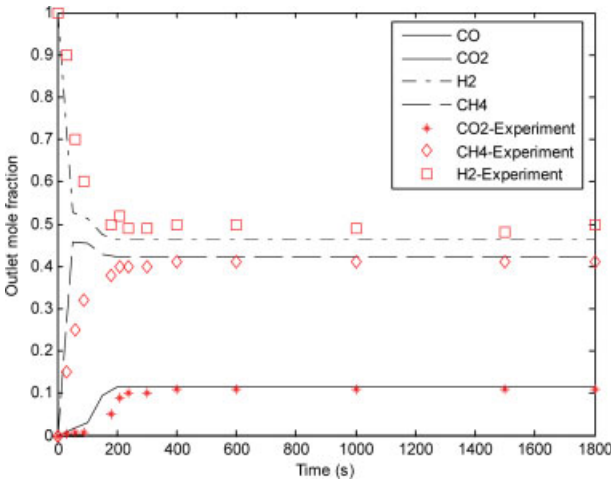

Figure 2. Effluent mole fraction on a water free basis for the reaction with sorption — process experimental data is taken from Ding and Alpay.[1]

Color figures can be viewed in the online issue, which is available at www.interscience.wiley.com.

reforming by Ding and Alpay.[11] Figures 2 and 3 show the mole fraction on water-free basis at the outlet of the reactor, with respect to time in the presence and absence of sorption enhancement, respectively. In the absence of sorption the time for the production of pure hydrogen is around 10 s, which is very less compared to the time of production of pure hydrogen from sorption enhanced reaction, approximately 250 s. Pure hydrogen has been defined as hydrogen with low-concentration of carbon oxides (less than 1%) on water-free basis. Hence, the overall productivity or yield of pure hydrogen is high when sorption is combined with reaction. The model results in Figures 2 and 3 are in excellent

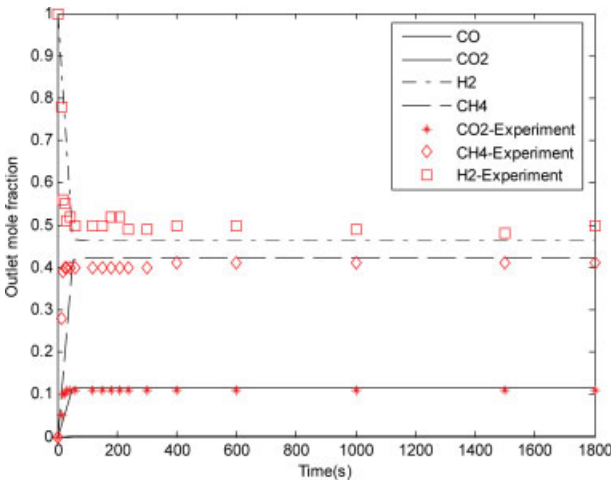

Figure 3. Effluent mole fraction on a water free basis for the reaction with sorption — process experimental data is taken from Ding and Alpay.[1]

Color figures can be viewed in the online issue, which is available at www.interscience.wiley.com.

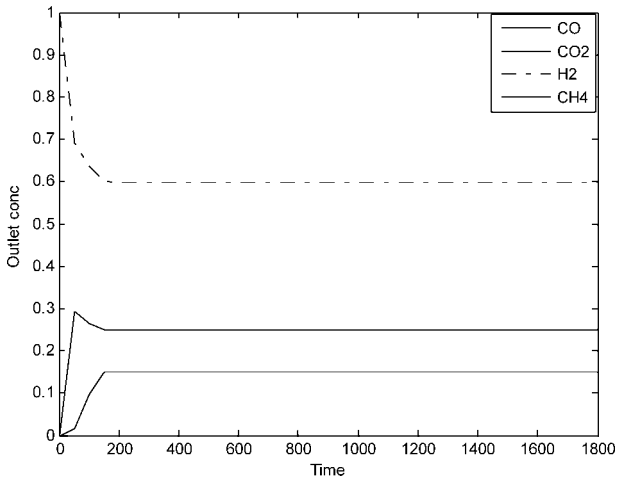

Figure 4. Mole fraction at the outlet of the reactor on a water-free basis with sorption for multifunctional particle.

agreement with the experimental data. The mole fraction at the outlet of the reactor on a water-free basis, using the heterogeneous simulation framework in Eqs. 5–9 for multifunctional particles with catalyst and sorbent functionalities is shown in Figure 4. The process conditions are kept the same as before, except η_j, which is set at 1.0. Here, the time for the production of pure hydrogen is approximately 100 s. This time has been reduced due to the consideration of heterogeneity and effects of diffusivity through particle pores, compared to the time obtained by considering homogeneous model in Figure 2. The yield of hydrogen can be calculated from the production of hydrogen for the total time period of operation of the reactor, or the time period where the quantity of carbon oxides is very low, which is dependent on the final application. The hydrogen produced for fuel cell applications should have a very low-concentration of carbon oxides, especially carbon monoxide which acts as a catalyst poison. For other applications, such as internal combustion engines the quantity of CO_2 should be controlled to reduce the greenhouse gas emission in the environment. However, for combined heat and power generating systems utilising hydrogen, yield is more important than purity. Based on the previous discussion, we can define two objective functions considering the tradeoffs between purity and productivity

$$\text{Objective function} = \int_0^t C_{H_2} dt \tag{19}$$

(a) *Yield*, where t = time to run a reactor. The time to run the reactor is decided, based on a desired purity of product or to exhaust the capacity of sorbent.

(b) *Yield1*, where t is the time for which concentration of CO_2 is lower than a certain threshold.

Characterization with homogeneous model

The sensitivity analysis is carried out with respect to bulk scale decision variables (Figure 1). The overall concentration of sorbent and catalyst decreases with increasing voidage. As

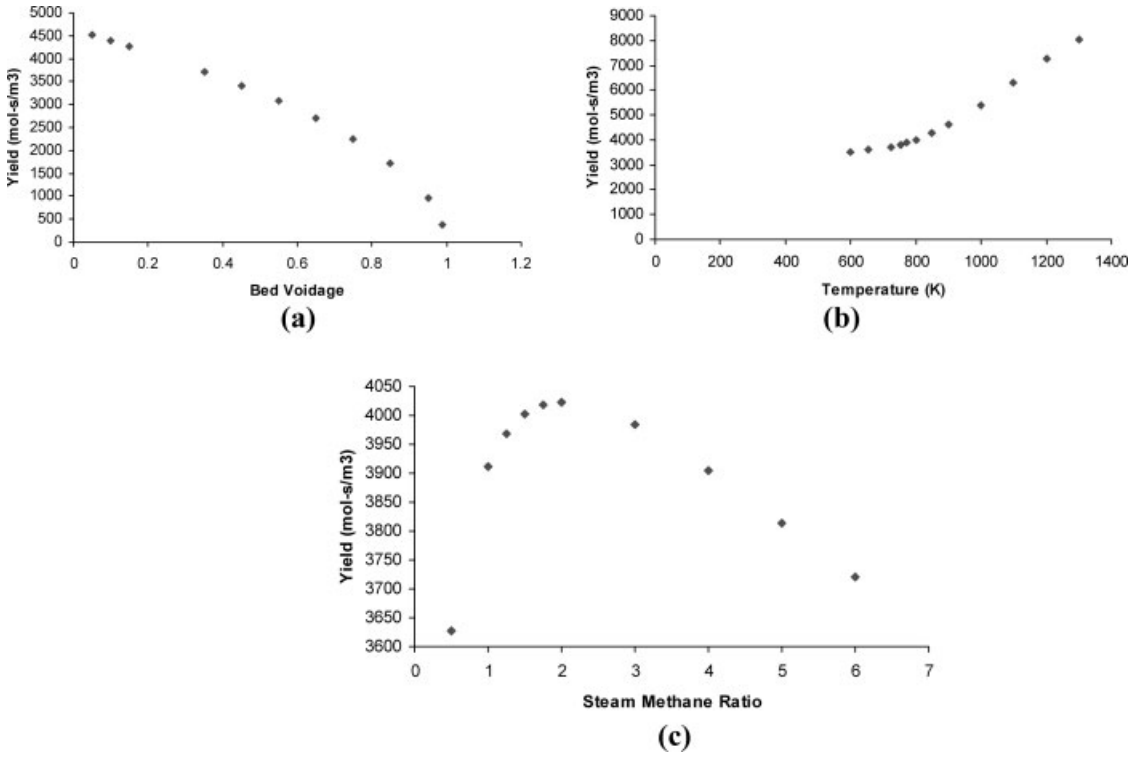

Figure 5. Effect of (a) bed voidage, (b) feed temperature, and (c) steam to methane ratio on the H2 yield.

a result the overall rate of reaction and sorption decreases (Figure 5a). By increasing the temperature the rate of forward reaction can be increased for the first two reactions in Eq 1. However, this decreases the rate of water-gas shift reaction (Eq 1, III). Consequently, by increasing the temperature, yield of H_2 is increased (Figure 5b). The maximum temperature permissible is limited by material of construction of the reactor. Decrease in the steam to methane ratio increases the reaction till a certain value, 2:1 in Figure 5c. However, lower steam to methane ratios favor soot and coke formation, which is not desirable for steam methane reforming process.[32] Steam to methane ratio of 4 to 6 is generally accepted in the industry. Hence, the steam to methane ratio is kept at a constant value of 6 for all further study. We can increase the time for production of hydrogen, and, hence, the yield or productivity of hydrogen by increasing the residence time for feed as presented Figure 6. The residence time can be increased by either increasing the length of reactor or decreasing the inlet velocity of stream.

Characterization with heterogeneous multiscale model

The system is a fixed-bed reactor containing multifunctional particles with integrated catalyst and sorbent functionalities. The parameters are specified in Appendix A. All the bulk level parameters, such as temperature, bed voidage and steam to methane ratio have the same effects as in the case of homogeneous system, studied in the previous section.

Particle level characterization

The ultimate objective of such intensified processes is to produce more pure hydrogen. However, the yield and purity of a product depend on design variables at reactor, as well as particle scales analyzed here. With increasing fraction of sorbent, the yield decreases while the purity of the product increases. The required purity of product depends on its end use. In the case study on steam methane reforming, if the hydrogen is to be used for fuel cell applications, the hydrogen produced should have very low-concentrations of carbon oxides especially carbon monoxide, as it acts as a catalyst poison. The amount of carbon monoxide for fuel cell applications should be less than 10 ppm.[32] The amount of CO obtained by the application of sorption enhanced reaction

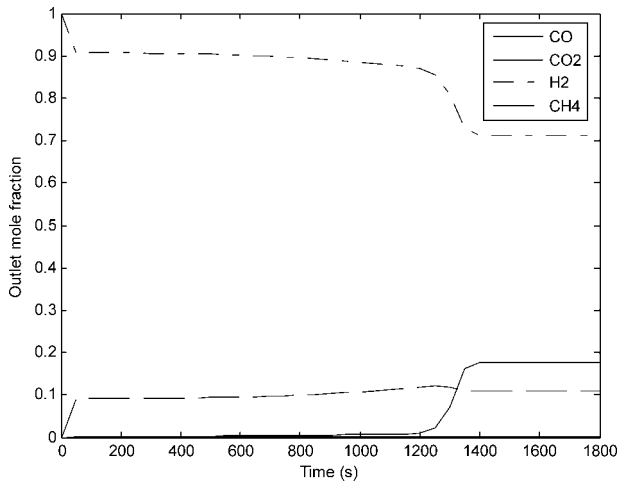

Figure 6. Mole fraction at the outlet of the reactor on a water-free basis with sorption with longer residence time.

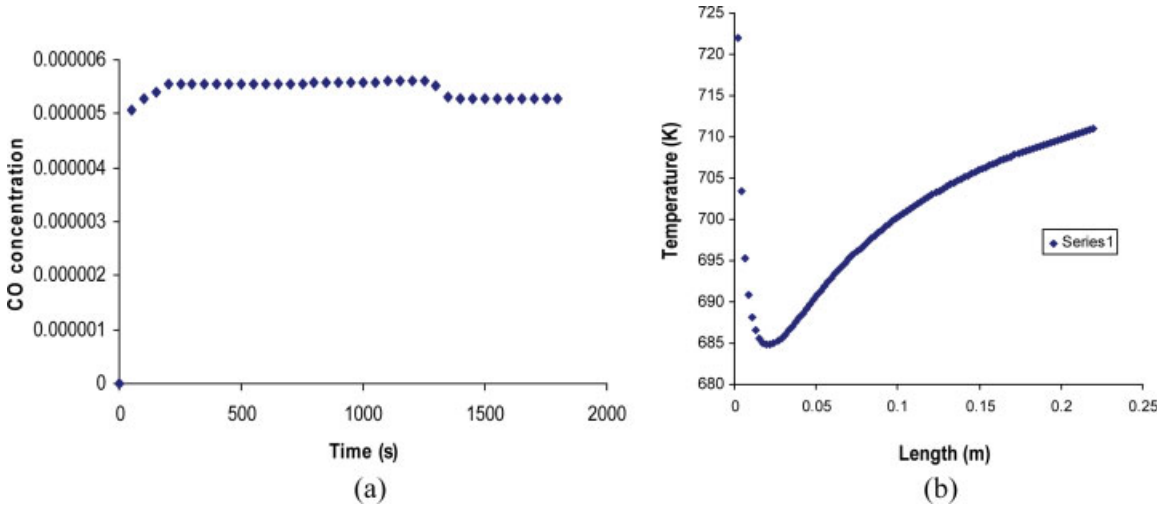

Figure 7. (a) Outlet concentration of CO, and (b) variation temperature along the length of the reactor.

Color figures can be viewed in the online issue, which is available at www.interscience.wiley.com.

process is approximately 5 ppm as provided in Figure 7a, which is within the allowable limit, when fully explored with the heterogeneous multiscale framework. Hence, the hydrogen produced is suitable for fuel cell applications. Figure 7b shows the variation of temperature along the length of the reactor. The wall temperature is maintained at the temperature of the feed. The feed entering the reactor consists of steam and methane, therefore, initially the first two endothermic reactions are predominant, and, hence, there is a drop in the temperature of the reactor. However, with an increase in concentration of CO and CO_2, there is an increase in the rate of exothermic reactions (water-gas-shift reaction and adsorption). Additionally, the temperature inside the reactor increases along the length of the reactor due to the heat transfer from the reactor wall in order to keep the wall temperature constant. Since adsorption is an exothermic process, and the conversion is increased by sorption, the reactor can be operated at a lower temperature than for the traditional SMR process for the same conversion.

If we increase the fraction of sorbent inside particles, the sorption of the product (CO_2) increases, and so does the rate of forward reaction according to the Le Chatelier's principle. However, this is at the cost of the concentration of catalyst inside particles that reduces the overall methane conversion. This offsets any increase in forward reaction, decreasing the overall hydrogen yield as shown in Figure 8. Therefore, we use *Yield1* in Eq. 19 as a measure of the quantity of pure hydrogen, devoid of oxides of carbon. Alongside, the time in which pure hydrogen can be produced and the quantity of pure hydrogen have been plotted against the fraction of sorbent in Figure 8. Both time and quantity of pure hydrogen increase with the increasing fraction of sorbent. Figure 8 also presents an important trade-off between hydrogen productivity and purity presented by *Yield* and *Yield1,* respectively, in Eq. 19. As discussed before, the objective function is decided based on the end use of a product. If the hydrogen produced is to be used for power generation we should work in zone I in Figure 8, however, for fuel cell applications, zone II should be the preferred region for deciding upon catalyst to sorbent ratio inside particles.

Additionally, multifunctional particles have other important design variables, such as particle voidage, diameter of particle, pore radius and tortuosity. Increase in the diameter of particle leads to decrease in yield due to increase in mass-transfer limitations as depicted in Figure 9. The effect of particle voidage on the yield in Figure 9b is due to the trade-off between decrease in mass-transfer limitation, and the reduction of active sites with increasing particle voidage.

Pore radius and tortuosity affect the diffusivity inside particle significantly, and, hence, the overall rate of reaction and sorption. We have used Thiele modulus to study the effects of these two parameters. Thiele modulus is the ratio of intrinsic chemical reaction/sorption rates without mass transfer to the rate of diffusion through a particle. The thiele modulus of reaction and sorption can be presented as in Eq. 20

$$\Phi_{cat,i} = R_p \sqrt{\frac{\overline{R_{cat,i}}}{d_i^{eff} \prod_i C_i^a}} \tag{20a}$$

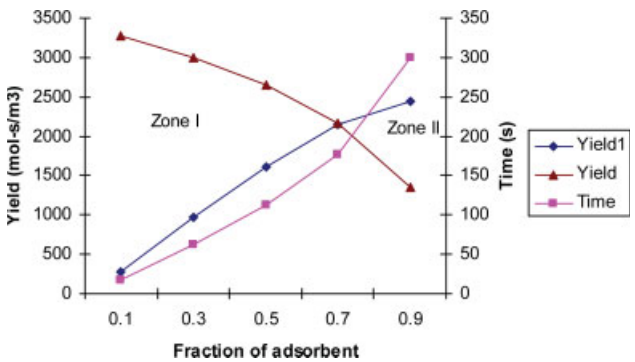

Figure 8. Effect of fraction of sorbent in a multifunctional particle on the yield and the time for production of pure hydrogen.

Color figures can be viewed in the online issue, which is available at www.interscience.wiley.com.

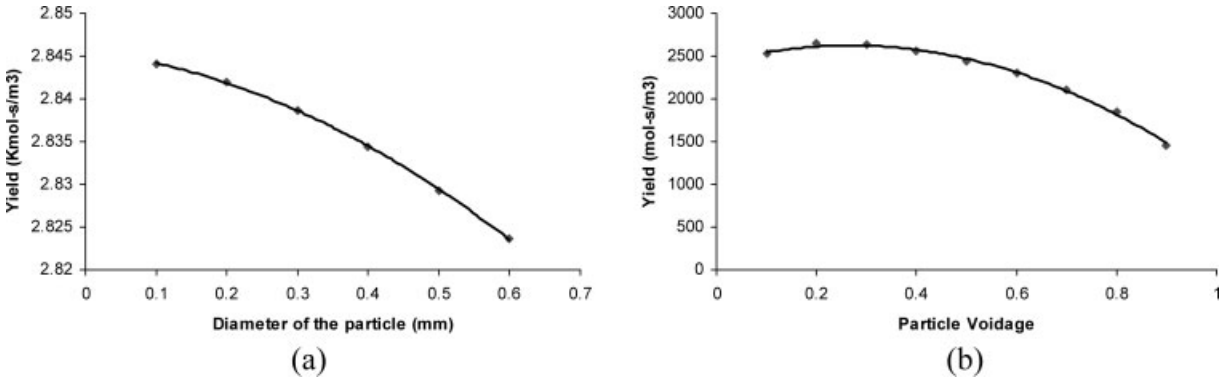

Figure 9. Effect of fraction of sorbent in multifunctional particle on the shield, and the time for production of hydrogen.

$$\Phi_{ads,i} = R_p \sqrt{\frac{\overline{R_{ads,i}}}{d_i^{eff} \prod_i C_i^a}} \tag{20b}$$

Figure 10a–d shows the variation in concentration with reaction Thiele modulus for H_2O, CO_2, H_2 and CH_4, respectively, for the various fractions of sorbent inside particles. The concentration of products increases along the length of a reactor, while that of the reactants decreases. Therefore, Thiele modulus decreases with increase in concentration of products and vice versa for reactants for a fixed catalyst to sorbent ratio inside particles. The increase in fraction of adsorbent inside the particle increases the concentration of products and the thiele modulus by increasing the rate of forward reaction. However, increase in concentration is not predominant for

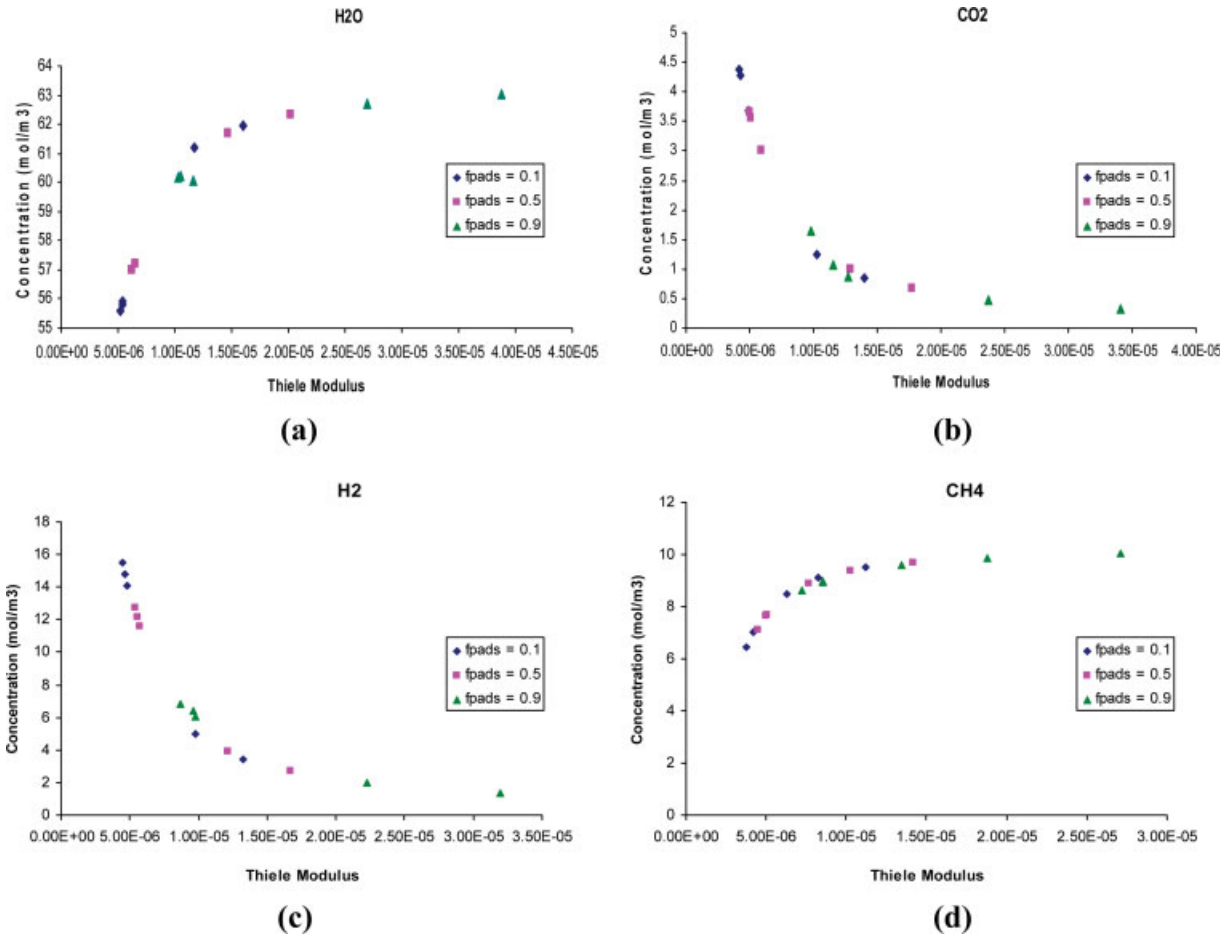

Figure 10. Thiele modulous $\Phi_{cat,i}$ with respect to concentration for different fraction of sorbent.

Color figures can be viewed in the online issue, which is available at www.interscience.wiley.com.

high-fraction of adsorbent, as there is a decrease in the amount of catalyst in the reactor. This is the same observation we made from Figure 8.

As shown in Eq. 10, effective particle diffusivity is a function of pore radius and tortuosity. If the ratio of pore radius to tortuosity is kept constant, concentration-Thiele modulus profiles inside reactors do not change as there is no change in the effective diffusivities of various components. The results are shown for the following combinations of pore radius and tortuosity, (a) $\bar{r} = 7 \times 10^{-9}$ $\tau_p = 4.3$ (base case), (b) $\bar{r} = 1.6 \times 10^{-8}$ $\tau_p = 8$ (coarser pore with highly constricted path), and (c) $\bar{r} = 1.7 \times 10^{-9}$ $\tau_p = 1$ (finer pore with even path).

Core-shell model

Dietrich et al.[21] selected a discrete set of particle structures, each representing the possible arrangements of catalyst and sorbent inside particle. They identified desired catalyst and sorbent arrangement inside particles for different reaction examples. We took into consideration three scenarios with different distribution of catalyst and sorbent inside particle as provided in Figure 11. We considered the fraction of catalyst and sorbent to vary linearly with the volume inside particle i.e.

$$f_{ads}^{p} = a + mr^3 \tag{21}$$

r varies between 0–1, and in this case is a ratio between the distance from the center of a particle divided by the radius of the particle, a and m are coefficients to be manipulated to find out the optimum arrangements.

The three different particle design arrangements are as follows. We examined their impact on *Yield1*, which is the amount of product produced. The basis of the calculation is the same as before, and given in Appendix A.

(a) high-fraction of sorbent in the outer shell, and low-fraction of sorbent in the core,

(b) High-fraction of catalyst in the outer shell, with high-fraction of sorbent in the core, and

(c) uniform ratio of catalyst and sorbent inside particles.

We compared these three cases with representative fractions indicated in Table 1. With catalyst in the shell and adsorbent in the core, initially the feed comes in contact with the catalyst shell, and the product is adsorbed at the adsorbent core. In the case of adsorbent shell and catalyst core, feed has to penetrate the depth of the particle to come in contact with the catalyst core, and the resultant product is then adsorbed in the shell. The mass transfer inside the particle poses a significant resistance to the reaction and separation process in the latter case. Hence, yield is higher if the catalyst is present in the outer shell compared to the other two cases, where the catalyst and sorbent fraction are uniform throughout, or the catalyst is present in the shell. The best shell-core arrangement of catalyst and sorbent is dependent on the type of reactions we handle. Further, optimization can be used along with the simulation, as discussed in this article, to fine-tune the various design variables for multifunctional catalysts, such as sorbent ratio, pore size and shape and core-shell arrangement.

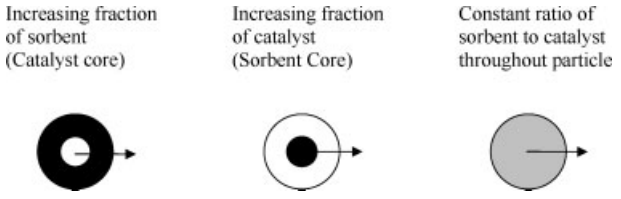

Figure 11. Three test scenarios.

Table 1. Yield of Pure Product for Different Representative Arrangements

Arrangement	Yield1	Fraction of adsorbent from shell to core				
Catalyst–core	8.732	0.8006	0.6137	0.4511	0.3229	0.2374
Sorbent–core	401.46	0.2994	0.4863	0.6489	0.7771	0.8626
Uniform mixture	150.76	0.5000	0.5000	0.5000	0.5000	0.5000

Regeneration. There are two possible approaches for regeneration of reaction adsorption bed : (a) Pressure swing adsorption,[4,6] and (b) Thermal swing adsorption.[33] The advantage of thermal swing adsorption is that it does not use rotating machinery (vacuum pump), and it does not use part of the product for pressurization, hence, more recovery of hydrogen.[33] In thermal swing, the reactor is pressurized and depressurized with the help of superheated steam at 590°C. Our model can be applied to regeneration processes using parameters that can be derived experimentally for these processes. Also to avoid the problem of coking we have fixed the steam to methane ratio at 6 as discussed earlier.

Conclusions

A heterogeneous multiscale framework has been developed that integrates transfer models at bulk and porous scales for *in situ* sorption enhanced reaction systems. The homogeneous models are first validated against experimental results and extended to heterogeneous framework. The productivity and purity tradeoffs are dependent on both reactor, as well as particle scale designs, such as bed voidage, temperature, steam to methane ratio, fraction of sorbent, particle voidage and ratio between porous radius and toruosity, etc. The catalyst and sorbent distribution inside particles strongly affects the purity and productivity tradeoffs. The respective zones dominated by productivity or purity were determined in terms of sorbent ratio inside particles for sorption enhanced natural gas reforming reaction producing pure hydrogen for combined heat and power and fuel cell applications, respectively. The yield of pure product can be increased by increasing the length of a reactor; however, such a design would lead to high-pressure drop and problems associated with regeneration of the sorbent. It was derived that the shell-core model with sorbent at the center of particles, and catalyst at the outer surface is better than the reverse design and the uniform catalyst and sorbent concentrations inside particles for the given reforming reaction. The particle-scale diffusion model considers the effects of porous diffusivity, which is a function of Knudsen diffusivity due to hindrance and molecular interactions, on particle-level transport. Moreover, two particle scale designs with (1) finer-even, and (2) coarser-constricted pores, have been considered to demonstrate that as long as the ratio between porous radius and tortuosity factor remain same, the outlet concentration or product yield does not change and varies only with catalyst to sorbent ratio inside particles.

Acknowledgment

Financial support from EPSRC (EP/D04829X/1) of the UK for undertaking this research is gratefully acknowledged.

Notation

b_{CO2} = Langmuir model constant for component CO_2, Pa^{-1}
$C_{f,i}$ = feed concentration of specie i, mol/m^3
C_i = concentration of specie i, mol/m^3
C_i^p = particle concentration of specie i, mol/m^3
C_i^{ic} = initial concentration of specie i, mol/m^3
Cp_g = specific heat of gas, J/mol-K
Cp_s = bulk specific heat, J/mol-K
C = overall concentration, mol/m^3
D_L = axial diffusion coefficient, m^2/s
D_m = molecular diffusion coefficient, m^2/s
d_p = diameter of particle, m
d_t = diameter of tube, m
d_i^{eff} = diffusivity inside particle of specie i, m^2/s
d_{ki}^e = Knudsen diffusivity of specie i, m^2/s
d_{im}^e = binary molecular diffusivity of specie i in specie m, m^2/s
E_{ad} = activation energy of sorption J/mol
f_{cat}^p = fraction of catalyst in the particle
f_{ads}^p = fraction of adsorbent in the particle
k = Boltzmann constant
$k(j)$ = forward rate of reaction j
$keq(j)$ = equilibrium constant for reaction j
$k_{ads,i}$ = rate constant of sorption
k_{ads,CO_2} = linear driving force mass-transfer coefficient
K_D, K_V = parameters in the Ergun correlation
L = length of the reactor
m_{CO2} = Langmuir model coefficient for component CO_2, mol/kg
Mw_i = molecular weight of specie i
M = average molecular weight
$nspc$ = total number of species
$nrxn$ = total number of reactions
$N_{p,i}^*$ = mass transfer into particle for specie i, mol/m^2-s
P = pressure, Pa
P_{CO} = partial pressure of CO, Pa
P_{CH4} = = partial pressure of CH_4, Pa
P_{CO2} = partial pressure of CO_2, Pa
P_{H2} = partial pressure of H_2, Pa
P_{H_2O} = partial pressure of H_2O, Pa
Pr = Prandtl number
q_i^* = equilibrium solid-phase concentration for specie i
q_i = sorbed-phase concentration for specie i
Re_p = Reynolds number
R = universal gas constant, J/mol-K
$r_{cat,j}$ = rate of reaction for jth reaction, mol/Kg-s
$\overline{R}_{cat,j}$ = average rate of reaction for jth reaction, mol/Kg-s
$r_{ads,i}$ = rate of sorption of specie i, mol/Kg-s
$\overline{R}_{ads,i}$ = average rate of sorption for specie i, mol/Kg-s
r = pore radius
r_p = particle radius
r = radius of particles
t = time, s
T = temperature, K
T_f = feed temperature, K
T_w = wall temperature, K
U = overall heat-transfer coefficient J/m^2-K
u = velocity, m/s
x = extent of sorption
y_{fi} = mole fraction of component i in the feed
y_i = mole fraction of specie i
z = axial length, m

Greek letters

ε = bed void fraction
ε_p = void fraction inside particle
ε_{im} = Lennard-Jones energy
τ_p = tortuosity
σ_{im} = characteristics length
$\Omega_{d_{im}}$ = diffusion collision integral
η_j = effectiveness factor for jth reaction
μ = viscosity
ρ_{ads} = density of sorbent, kg/m^3
ρ_{cat} = density of catalyst, kg/m^3
ρ_b = density of bed, kg/m^3
ρg = density of gas, kg/m^3
v_{ij} = stoichiometric coefficient for specie i in jth reaction
$\Delta w_{\max}$ = maximum experimental uptake of CO_2 by the sorbent
λ_z = effective axial conductivity
λ_g = gas conductivity
$\Delta H_{ads,i}$ = heat of sorption of specie i, J/mol
$\Delta H_{R,j}$ = heat of jth reaction, J/mol
$\Phi_{cat,i}$ = Thiele modulus of catalysis for specie i
$\Phi_{ads,i}$ = Thiele modulus of sorption for specie i

Literature Cited

1. Agar DW, Ruppel W. Multifunktionale reaktoren fdr die heterogene Katalyse. *Chem Eng Technol*. 1988;60:731.
2. Krishna R. Reactive separations: more ways to skin a cat. *Chem Eng Sci*. 2002;57:1491.
3. Armor JN. Membrane catalysis: Where is it now, what needs to be done? *Catalysis Today*. 1995;25(3–4):199–207.
4. Hufton JR, Mayorga S, Sircar S. Sorption-enhanced reaction process for hydrogen production. *AIChE J*. 1999;45(2):248–256.
5. Hufton J, Waldron W, Weigel S, Rao M, Nataraj S, Sircar S. Sorption Enhanced Reaction Process (SERP) for the Production of Hydrogen. Paper presented at: Proceedings US DOE Hydrogen Program Review; 2000.
6. Carvill BT, Hufton JR, Anand M, Sircar S. Sorption-enhanced reaction process. *AIChE J*. 1996;42(10):2765–2772.
7. Waldron WE, Hufton JR, Sircar S. Production of hydrogen by cyclic sorption enhanced reaction process. *AIChE J*. 2001;47(6):1477–1479.
8. Harrison DP, Peng Z. Low-carbon monoxide hydrogen by sorption-enhanced reaction. *Int J of Chem Reactor Eng*. 2003;1(A37):1–9.
9. Lopez Ortiz A, Harrison DP. Hydrogen production using sorption-enhanced reaction. *Ind Eng Chem Res*. 2001;40(23):5102–5109.
10. Lyon RK, Cole JA. Unmixed combustion: an alternative to fire. *Combustion and Flame*. 2000;121(1–2):249–261.
11. Ding Y, Alpay E. Adsorption-enhanced steam-methane reforming. *Chem Eng Sci*. 2000;55(18):3929–3940.
12. Ding Y, Alpay E. Equilibria and kinetics of CO_2 adsorption on hydrotalcite adsorbent. *Chem Eng Sci* 2000;55:3461.
13. Wang Y-N, Rodrigues AE. Hydrogen production from steam methane reforming coupled with in situ CO_2 capture: Conceptual parametric study. *Fuel*. 2005;84(14–15):1778–1789.
14. Xiu G-h, Soares JL, Li P, Rodrigues AE. Simulation of five-step one-bed sorption-enhanced reaction process. *AIChE J*. 2002;48(12):2817–2832.
15. Xiu G-h, Li P, Rodrigues AE. New generalized strategy for improving sorption-enhanced reaction process. *Chem Eng Sci*. 2003;58(15):3425–3437.
16. Xiu G, Li P, Rodrigues AE. Adsorption enhanced steam methane reforming with intrapartile diffusion limitations. *Chem Eng J*. 2003;95:83–93.
17. Koumpouras GC, Alpay E, Lapkin A, Ding Y, Frantisek S. The effect of adsorbent characteristics on the performance of a continuous sorption-enhanced steam methane reforming process. *Chem Eng Sci*. 2007; In Press.
18. Koumpouras GC, Alpay E, Stepanek F. Mathematical modelling of low-temperature hydrogen production with in situ CO2 capture. *Chem Eng Sci*. 2007;62(10):2833–2841.
19. Koumpouras GC, Alpay E, Lapkin A, Ding Y, Stepanek F. The effect of adsorbent characteristics on the performance of a continuous sorption-enhanced steam methane reforming process. *Chem Eng Sci*. In Press.
20. Elsner MP, Dittrich C, Agar DW. Adsorptive reactors for enhancing equilibrium gas-phase reactions--two case studies. *Chem Eng Sci*. 2002;57(9):1607–1619.
21. Dietrich W, Lawrence PS, Grunewald M, Agar DW. Theoretical studies on multifunctional catalysts with integrated adsorption sites. *Chem Eng J*. 2005;107(1–3):103–111.

22. Rusten HK, Ochoa-Fernandez E, Chen D, Jakobsen HA. Numerical Investigation of Sorption Enhanced Steam Methane Reforming Using Li2ZrO3 as CO2-acceptor. *Ind Eng Chem Res*. 2007;46(13): 4435–4443.
23. Danckwerts PV. Continuous flow systems : Distribution of residence times. *Chem Eng Sci*. 1953;2(1):1–13.
24. Sankararao B, Gupta SK. Modeling and simulation of fixed bed adsorbers (FBAs) for multi-component gaseous separations. *Comp & Chem Eng*. In Press.
25. Treybal RE. *Mass-Transfer Operations*. 2nd ed. New York: McGraw-Hill; 1968.
26. Poling BE, Prausnitz JM, O'Connell JP. *The properties of gases and liquids*. 5th ed. New York: McGraw-Hill; 2001.
27. Edwards MF, Richardson JF. Gas dispersion in packed beds. *Chem Eng Sci*. 1968;23(2):109–123.
28. Ergun S. Flow through packed columns. *Chem Eng Progress*. 1952;48(2):89.
29. Yagi S, Kunii D, N. W. Studies on axial effective thermal conductivities in packed beds. *AIChE J*. 1960;6(4):543–546.
30. Dixon AG, Ertan Taskin M, Hugh Stitt E, Nijemeisland M. 3D CFD simulations of steam reforming with resolved intraparticle reaction and gradients. *Chem Eng Sci*. 2007;In Press.
31. Xu J, Froment GF. Methane steam reforming, methanation and wate-gas shift: I. Intrinsic kinetics. *AIChE J*. 1989;35:88–97.
32. Ersoz A, Olgun H, Ozdogan S. Reforming options for hydrogen production from fossil fuels for PEM fuel cells. *J of Power Sources*. 2006;154(1):67–73.
33. Lee KB, Beaver MG, Caram HS, Sircar S. Novel thermal-swing sorption-enhanced reaction process concept for hydrogen production by low-temperature steam-methane reforming. *Ind Eng Chem Res*. 2007;46(14):5003–5014.
34. Xiu G, Soares JL, Li P, Rodrigues AE. Simulation of five step one bed sorption enhanced reaction process. *AIChE J*. 2002;48:2817.

Appendix A: Parameters Used in the Simulation

$C_{f,CO_2} = 0$ (Ding and Alpay[11])
$C_{f,CH_4} = 10.3643$ mol/m^3(Ding and Alpay[11])
$C_{f,H_2O} = 63.6664$ mol/m^3(Ding and Alpay[11])
$C_{f,CO} = 0$ (Ding and Alpay[11])
$C_{f,H_2} = 0$ (Ding and Alpay[11])
$C^{ic}_{CO_2} = 0$ (Guo-Hua Xiu[34])
$C^{ic}_{CH_4} = 0$ (Guo-Hua Xiu[34])
$C^{ic}_{H_2O} = 71.8098$ mol/m^3 (Guo-Hua Xiu[34])
$C^{ic}_{CO} = 0$ (Guo-Hua Xiu[34])
$C^{ic}_{H_2} = 2.2209$ mol/m^3 (Guo-Hua Xiu[34])
$Cp_g = 42$ J/mol-K
$Cp_s = 850$ J/mol-k
$D_p = 3.3 \times 10^{-7}$ m^2/s(Guo-Hua Xiu[34])
$d_p = 3.57 \times 10^{-4}$ m (Guo-Hua Xiu[34])
$d_t = 5 \times 10^{-2}$ m (Ding and Alpay[11])
$D_m = 1.6 \times 10^{-5}$ m^2/s (Guo-Hua Xiu[34])
$f^p_{ads} = 0.4$
$\Delta H_{ads,CO2} = -17$ KJ (Guo-Hua Xiu[34])
$\Delta H_{R,\ I,\ 298} = 206.2$ KJ/mol (Xu and Froment[31])
$\Delta H_{R,\ II,\ 298} = 164.9$ KJ/mol (Xu and Froment[31])
$\Delta H_{R,\ III,\ 298} = -41.1$ KJ/mol (Xu and Froment[31])
$L = 0.22$ m (Ding and Alpay[11])
$m_{CO_2} = 0.65$ mol/kg (Ding and Alpay[11,12])
$P = 445.7$ KPa (Guo-Hua Xiu[34])
$\rho_{\text{cat}} = 139$ kg/m^3 (Guo-Hua Xiu[34])
$\rho_{\text{ads}} = 609$ kg/m^3(Guo-Hua Xiu[34])
$\rho_g = 1$ kg/m^3
$\bar{r} = 710^{-9}$ m
$T_f = 723$ K (Guo-Hua Xiu[34])
$T_w = 730$ K (Guo-Hua Xiu[34])
$\tau_p = 4.298$
$u = 0.13$ m/s (Ding and Alpay[11,12])
$U = 71$ J/m^2−K (Guo-Hua Xiu[34])
$\mu = 2.8710^{-5}$ Pa-s
$\varepsilon = 0.35$ (Ding and Alpay[11])
$\varepsilon_p = 0.24$ (Ding and Alpay[11])

Sets

nspc = {*i, m*/species}
nrxn = {*j*/reaction I, II, III}

Manuscript received May 26, 2007, and revision received Dec. 12, 2007.